High-field phase diagram of the heavy-fermion metal $CeIn_3$: Pulsed-field NMR study on single crystals up to 56 T

Y. Tokunaga,[1,*] A. Orlova,[2] N. Bruyant,[2] D. Aoki,[3,4] H. Mayaffre,[2] S. Krämer,[2] M.-H. Julien,[2] C. Berthier,[2] M. Horvatić,[2] N. Higa,[1] T. Hattori,[1] H. Sakai,[1] S. Kambe,[1] and I. Sheikin[2]

[1]*ASRC, Japan Atomic Energy Agency, Tokai, Ibaraki 319-1195, Japan*

[2]*LNCMI-CNRS (UPR 3228), EMFL, UGA, UPS, INSA, 31400 Toulouse and 38042 Grenoble, France*

[3]*INAC/PHELIQS, CEA-Grenoble/UGA, 38000, Grenoble, France*

[4]*IMR, Tohoku University, Oarai, Ibaraki 311-1313, Japan*

(Received 25 November 2018; revised manuscript received 5 February 2019; published 28 February 2019)

The heavy-fermion antiferromagnet $CeIn_3$ exhibits a field-induced anomaly associated with Fermi surface reconstruction at $H^* \sim 45$ T, well below the antiferromagnetic (AFM) critical field that exceeds 60 T. In order to explore the origin of this anomaly, we have measured ^{115}In NMR spectra in pulsed magnetic fields up to 56 T using high-quality single crystals. To within experimental resolution, we do not detect any change in the NMR spectra that could suggest a modification in either the character of the hyperfine field or the electric field gradient at In sites through H^*. This strongly suggests that the 45 T anomaly cannot be simply ascribed to a field-induced change in the magnetic structure of the AFM state. Neither do we find any evidence of changes in the crystallographic structure or in the distribution of charge density at H^*. The field dependence of the NMR shift implies the existence of a field-induced anomaly in the hyperfine coupling above H^*.

DOI: 10.1103/PhysRevB.99.085142

I. INTRODUCTION

$CeIn_3$, which crystallizes into a simple cubic crystal structure [1,2], is one of the simplest and best-studied heavy-fermion (HF) compounds. At ambient pressure and zero magnetic field, it exhibits antiferromagnetic (AFM) order below $T_N = 10$ K. $CeIn_3$ is one of the first HF materials, in which a small dome of superconductivity was observed around a pressure-induced quantum phase transition (QPT) from AFM to a paramagnetic (PM) phase at $P_c \approx 2.6$ GPa [1]. More recent experimental studies demonstrated that the AFM order can be also suppressed by a magnetic field (H), in which a field-induced QPT occurs at the critical field H_c, which varies from 60 to 80 T, depending on the field orientation (Fig. 1) [3–5]. The exact nature of the field-induced QPT remains poorly understood, and is less well studied than the pressure-tuned QPT. This is partly due to the limited number of experimental techniques available at very high magnetic fields. Nevertheless, several experiments performed in pulsed magnetic fields suggest different ways of approaching pressure- and field-tuned QPTs [4,5].

A QPT is not the only feature induced in $CeIn_3$ by high magnetic fields. Indeed, a clear anomaly was discovered in tunnel diode oscillator (TDO) measurements [6] at $H^* \sim 45$ T, well below H_c (Fig. 1). Surprisingly, a corresponding anomaly was not observed in resistivity measurements [5]. The physical origin of this transition, or crossover, is at present obscure. Interestingly, small heavy f-hole pockets of the Fermi surface observed at low magnetic fields disappear at about H^* [7]. These small pockets are not observed in the PM state induced by either pressure [8] or magnetic field [4], and are not predicted by band-structure calculations [8]. Therefore, they are likely to originate from the fragmentation of the large Fermi surface that exceeds the size of the antiferromagnetic Brillouin zone. Remarkably, a similar anomaly in TDO measurements was recently observed in $CePt_2In_7$ at about the same field, where a similar change in the Fermi surface was also reported [9]. Furthermore, in $CePt_2In_7$, an anomaly in magnetic torque measurements has been observed at exactly the same field [10], implying that the 45 T transition, or crossover, could be associated with a change of magnetic properties.

A possible explanation for the feature observed at 45 T in both $CeIn_3$ and $CePt_2In_7$ is a field-induced change of the magnetic and/or crystal structure, which may occur at H^*. Indeed, a modification of the magnetic and/or crystal structure leads to a change of the (magnetic) Brillouin zone and, therefore, to a Fermi surface modification. Another, more exciting possibility, is that the 45 T anomaly corresponds to a field-induced transition to a density-wave state, as was recently proposed for the sister compound $CeRhIn_5$ [11], in which such a transition occurs at 30 T.

More recently, however, Moll *et al.* suggested that a level crossing of the Γ_7 doublet ground state and the Γ_8 quartet excited state of the Ce $4f$ wave function occurs at around 45 T [5]. This assumption is supported by mean-field calculations allowing for cubic anisotropy in the exchange interactions, which suggests that the effect is necessary to explain the measured anisotropy of the H-T phase diagram in high fields. This implies that the 45 T anomaly in the Fermi surface can be also associated with a field-induced change of the orbital character of the Ce $4f$ wave function.

These possible origins of the 45 T transition, or crossover, in $CeIn_3$ motivated us to perform a high-magnetic-field NMR study using a pulsed magnet.

*tokunaga.yo@jaea.go.jp

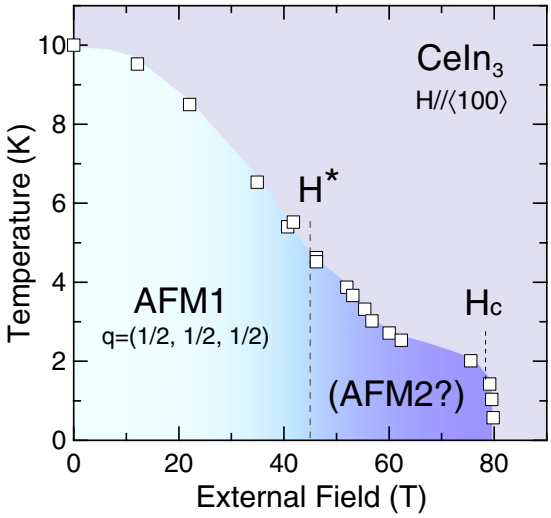

FIG. 1. Temperature–magnetic-field phase diagram for fields applied along the ⟨100⟩ direction in $CeIn_3$ [5]. An anomaly was observed in TDO measurements at $H^* \approx 45$ T [6].

In this paper, we report ^{115}In-NMR measurements in a high-quality single crystal of $CeIn_3$ at fields up to 56 T. We find that the essential features of the NMR spectra do not change across H^*. This suggests that the anomaly at H^* cannot be simply accounted for by a field-induced change of the magnetic structure in the AFM state.

II. EXPERIMENTAL RESULTS AND DISCUSSION

A. Single crystal

All the measurements reported here were performed on high-quality $CeIn_3$ single crystals grown by the self-flux method. In order to minimize unavoidable heating of metallic crystals by eddy currents under pulsed magnetic fields, a single crystal of the size of $2 \times 2 \times 6$ mm^3 was sliced into four $\sim$0.5-mm plates, which were restacked and intercalated by thin insulating tapes. The slicing of the crystal also offers an advantage for the NMR signal detection by increasing the crystalline surface area.

B. Field-swept NMR spectrum

In Fig. 2 we show lower-field ^{115}In NMR spectra obtained on our single crystal for (a) PM and (b) AFM states, respectively. The data were obtained below 15 T using a superconducting magnet at the Laboratoire National des Champs Magnétiques Intenses (LNCMI) in Grenoble. The magnetic field was applied parallel to the ⟨100⟩ axis of the cubic structure. Within the cubic $AuCu_3$-type structure of $CeIn_3$, all the In sites are equivalent in zero field (Fig. 3). However, since the direction of the local electric field gradient (EFG) principal axis V_{zz} is perpendicular to the plane of the four nearest-neighbor Ce atoms, the In ions split into two inequivalent sites with different θ for $H \| \langle 100 \rangle$. Here, θ is the angle between V_{zz} and H. In a unit cell, two of six In sites have $\theta = 0^\circ$ [(1) and (2) in Fig. 3], while the others have $\theta = 90^\circ$ [(3)–(6) in Fig. 3]. The former are labeled as $In^{\|}$ and the latter as $In^{\perp}$ throughout this paper. In addition, each In site gives rise

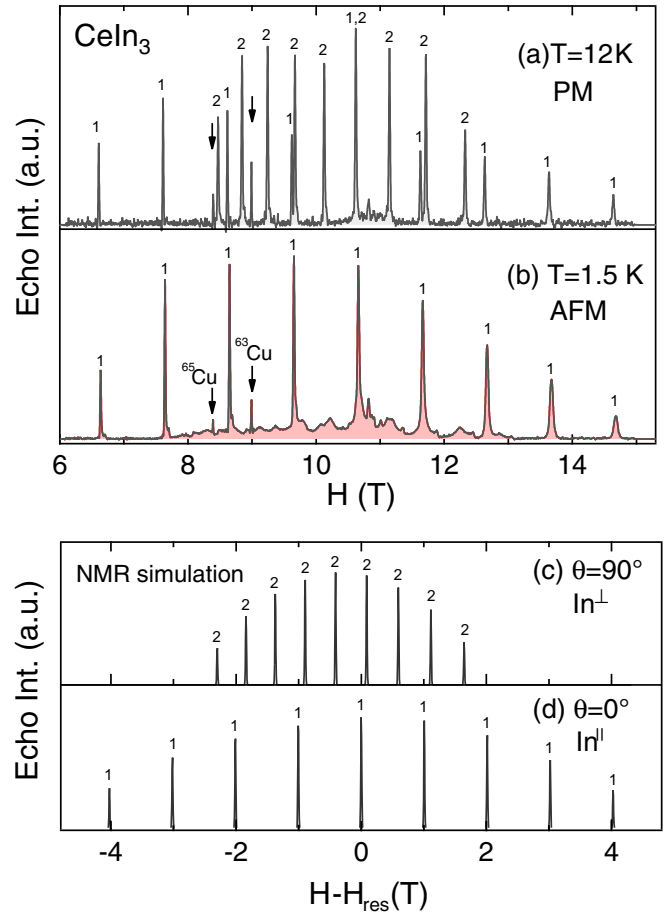

FIG. 2. The field-swept ^{115}In NMR spectra obtained in (a) PM and (b) AFM states in fields below 15 T. Here the spin-echo signals were recorded at a fixed frequency of 101.8 MHz by changing H in equally spaced steps. The spectra were then obtained by adding the Fourier transforms of spin-echo signals at each field value. The spectrum in the PM state consists of two sets of sharp peaks; one set separated by about 1 T (labeled 1), the other separated by about 0.5 T (labeled 2). On the other hand, the spectrum in the AFM state contains only nine sharp peaks separated by about 1 T. In the lower panel, we show the results of numerical simulations for (c) $In^{\perp}(\theta = 90^\circ)$ and (d) $In^{\|}(\theta = 0^\circ)$. The numerical simulations were performed using a diagonalized total Hamiltonian matrix consisting of EFG and Zeeman terms, where the EFG parameters are fixed at $\nu_Q = 9.61$ MHz and $\eta = 0$, respectively [12–15]. The simulations include the effect of the hyperfine field due to the field-induced magnetization along the field direction, shown in Fig. 6.

to nine separate peaks owing to quadrupolar splitting of the nuclear spin $I = 9/2$. The EFG parameters $\nu_Q = 9.61$ MHz and $\eta = 0$ can be expected according to the previous NQR measurements [12–15]. The NMR line splitting of about 0.5 and 1 T is observed for the $In^{\perp}$ and the $In^{\|}$ sites, respectively [Figs. 2(c) and 2(d)]. Thus, the observed spectrum in the PM state is well explained as a superposition of two sets of nine satellite peaks arising from $In^{\perp}$ and $In^{\|}$ sites, as seen in Fig. 2(a).

On the other hand, only nine sharp peaks arising from the $In^{\|}$ sites are detectable in the AFM state [Fig. 2(b)]. The peaks from $In^{\perp}$ sites are all broadened out due to the

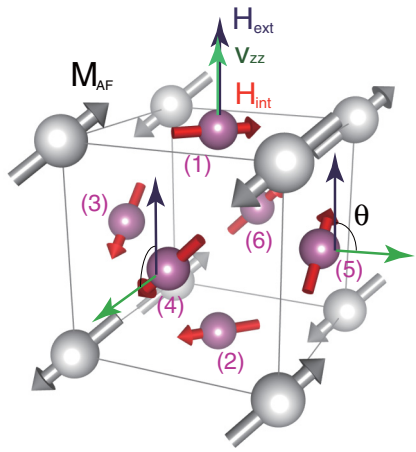

FIG. 3. Crystal and magnetic structures of $CeIn_3$. The local symmetry of the In site is tetragonal, and therefore the asymmetry parameter of the EFG is $\eta = 0$. The local principal axis of the EFG (V_{zz}) for each In site, denoted by a green arrow, is perpendicular to the plane of the four nearest-neighbor Ce atoms. The direction of the applied field H is denoted by black arrows. θ is the angle between V_{zz} and H. Below $T_N = 10$ K, Ce moments (M_{AF}) order antiferromagnetically with the zero-field propagation vector (1/2, 1/2, 1/2) [16], which generates hyperfine fields H_{hf} (red arrows) parallel to the Ce-In plane [12]. The numbering scheme shown for In sites is referenced in the text.

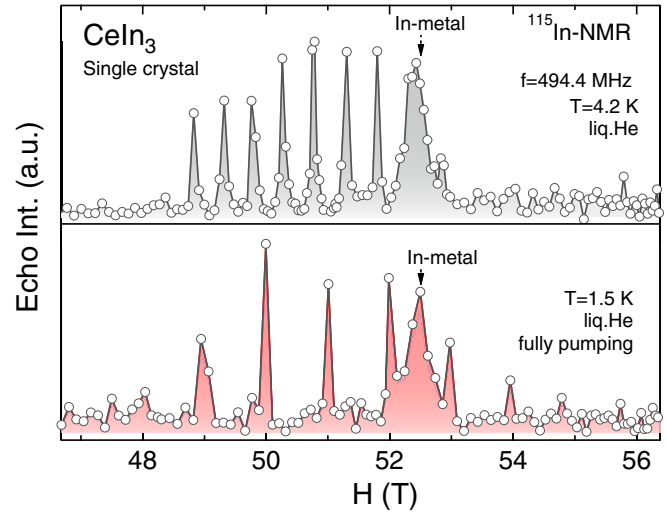

FIG. 4. Temperature dependence of the field-swept NMR spectrum obtained in the pulsed magnet with a fixed NMR frequency 494.4 MHz.

hyperfine field H_{hf} that appears parallel to the Ce nearest-neighbor (Ce-NN) planes at In sites. Namely, when $H \gg H_{hf}$, the H_{hf} perpendicular to the direction of the quantization axis of the nuclear spins ($\|H$) does not contribute to NMR line broadening. This result is consistent with the previous NQR studies, which suggest $H_{hf} \sim 0.6$ T lying in the Ce-In plane [12–15]. In the AFM state, Ce moments (M_{AF}) order along ⟨111⟩, with the propagation vector (1/2, 1/2, 1/2) [16]. Based on the symmetry considerations, one might suppose that the transferred hyperfine field from four Ce-NN moments are all canceled out at In sites (see Fig. 3). Indeed, our measurements demonstrate that most of the transferred hyperfine fields are canceled out at In sites, although a small H_{hf} lying in the Ce-In plane remains. This nonvanishing H_{hf} is present since the transferred hyperfine couplings are symmetric with respect to the bond axes rather than crystal lattice directions, as discussed in the case of $CeTIn_5$ [17].

C. NMR in pulsed magnetic fields

Next we discuss the results of the pulsed-field NMR [18–25]. The pulsed-field NMR experiments were performed using a homogeneous pulsed-field, 60-T magnet (with 70 ms rise time) at the LNCMI in Toulouse [24]. The field was applied parallel to the ⟨100⟩ direction. The ^{115}In nuclei possess a high nuclear spin value ($I = 9/2$) with a relatively large nuclear gyromagnetic ratio ($\gamma_N/2\pi = 9.3295$ MHz/T) and a large natural abundance (95.7%), providing high-sensitivity NMR detection. This allows us to detect NMR spin echoes without signal averaging. During a magnetic-field pulse, the echo-pulse sequence consisting of 1.5 and 3 μs excitation pulses separated by 4 μs was repeated continually every 200 μs. The full NMR spectrum was then constructed by plotting the integrated intensities of recorded spin-echo signals against the average value of the time-dependent H during each echo-pulse sequence. For each pulse of the magnetic field, a field profile was recorded by measuring the voltage of a pick-up coil. To gain higher accuracy of absolute field values, we renormalized the profile using ^{63,65}Cu and ^{115}In NMR signals arising from a metallic copper and indium powder samples placed in the same NMR coil as the $CeIn_3$ sample. The Knight shifts of metallic copper and indium, $^{63,65}K = 0.238\%$ and $^{115}K = 0.81\%$, were used for the corrections [26].

Figure 4 shows pulsed-field ^{115}In NMR spectra measured at a constant NMR frequency (f_{NMR}) of 494.4 MHz, where the crystals are cooled (a) in liquid ^{4}He (4.2 K), and (b) at the base temperature of the pumped ^{4}He cryostat (1.5 K), respectively. A clear change in the NMR spectrum confirms that a magnetic phase transition from PM to AFM states occurs between the two temperatures. This result agrees with the high-field phase diagram of $CeIn_3$ constructed from resistivity measurements (Fig. 1), which yields the estimated value of $T_N \sim 4$ K at $H \sim 50$ T [5]. Conversely, the change in the spectrum observed here ensures that our metallic crystal in the pumped ^{4}He cryostat (i.e., with superfluid ^{4}He) stayed low enough below $\sim$4 K to yield stable AFM behavior, despite possible heating due to the high-field pulse. However, we cannot rule out the possibility of approaching, or even crossing, the AFM-PM transition at 56 T, the highest field of our measurements, where the transition occurs slightly above 2 K.

In Figs. 5(a)–5(c), we compare the AFM ordered state spectra obtained in three different field regions. To make the comparison easier, the field axis is centered on H_{res} in each case, with a scan range of $\pm$4.5 T. H_{res} is the resonance field of the central peak in each spectrum, having the values (a) $H_{res} = 10.7$ T, (b) 36.4 T, and (c) 52 T. The scan range for (a) and (b) is thus confined to the region below H^*, while for (c) it lies entirely above H^*. Although the resolution is diminished in the pulsed-field spectra [(b) and (c)], it is recognized that the spectral structure is well preserved in all the field

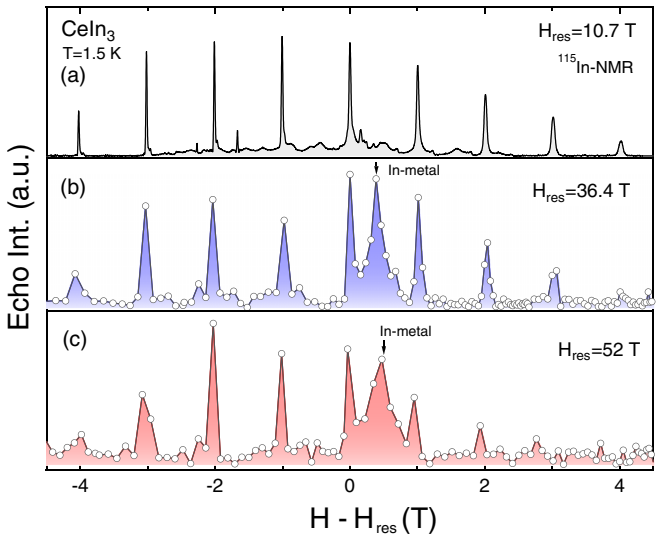

FIG. 5. Field dependence of the NMR spectrum. The horizontal axis is $\Delta H = H_{\rm ext} - H_{\rm res}$, where $H_{\rm res}$ is the field value of the central peak in each spectrum, i.e., (a) 10.7 T, (b) 36.4 T, and (c) 52 T, respectively.

regions through H^*. This shows clearly that there is no change in the lattice symmetry or parameter, since the EFGs that are critically dependent on those elements are not modified in any way. Furthermore, the absence of a considerable broadening or splitting of NMR lines above H^* suggests that the major cancellation of the transferred hyperfine fields from Ce-NN moments are still preserved. Namely, there is no signature of the change of the magnetic structure above H^*. More precisely, the spectra exclude any onset of AFM structures providing staggered components of $H_{\rm int}$ along the field direction. There is no sign of incommensurability of the magnetic structure above H^* either. A magnetic-field-induced density-wave scenario is also unlikely; however, we do not completely rule out this possibility since the resolution of our pulsed-field NMR spectra (about 0.5–1 kOe) might be not high enough to resolve a small change of the NMR linewidth or splitting.

Finally, in Fig. 6 we plot the field dependence of the NMR shift, $\Delta H^{\parallel} = H_{\rm bare} - H_{\rm res}$, where $H_{\rm bare} = f_{\rm NMR}/^{115}\gamma$. When

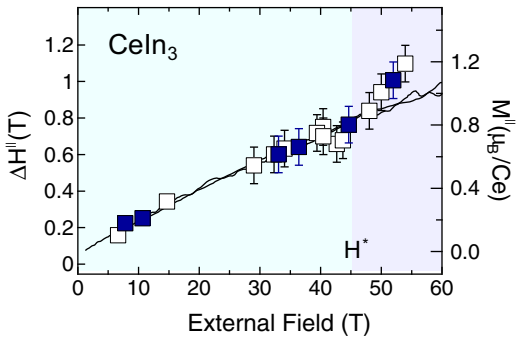

FIG. 6. Field dependence of the NMR shift, $\Delta H^{\parallel} = H_{\rm bare} - H_{\rm res}$ plotted together with the magnetization, $M^{\parallel}$, of a powder sample cited from Ref. [3] (solid line, right vertical axis). The $H_{\rm res}$ values were extracted from the field values of the center (solid square) and satellite (open square) peaks in several NMR spectra measured in different field regions.

$H \gg H_{\rm hf}$, $\Delta H^{\parallel}$ corresponds to the component of the hyperfine field induced parallel to H, and hence it is proportional to field-induced magnetization along the field direction $M^{\parallel}$, i.e., $\Delta H^{\parallel} \simeq A^{\parallel}_{\rm hf} M^{\parallel}$, where the $A^{\parallel}_{\rm hf}$ is the hyperfine coupling constant between Ce $4f$ moments and In nuclei. In the figure, we also plot $M^{\parallel}$ measured by Ebihara *et al.* in a powder sample of $CeIn_3$ [3]. In the AFM state, the $M^{\parallel}$ is associated with the expected canting of the AFM sublattices toward the applied field as it increases. It shows clearly that those sublattices are the source of a positive transferred shift field at the In sites.

As seen in Fig. 6, the field dependence of $\Delta H^{\parallel}$ deviates from that of $M^{\parallel}$ above $H^* \simeq 45$ T. This implies the existence of a field-induced anomaly in $A_{\rm hf}$ above H^*. Here, the hyperfine coupling is dominated by an indirect mechanism mediated by the orbital hybridizations between Ce and In atoms [17]. Therefore, a possible origin of the anomaly is a change of the orbital character of the Ce $4f$-wave functions driven by the crystal field-level crossing. Moll *et al.* suggested that the level crossing of the Γ_7 doublet ground state and the Γ_8 quartet excited state occurs around 45 T for $H \| \langle 100 \rangle$ [5]. Our results are indeed compatible with this scenario. It should be also noted that up to now, high-field magnetization measurements have been performed only on powder samples of $CeIn_3$. Therefore, the mismatch between the H dependence of $\Delta H^{\parallel}$ and $M^{\parallel}$ might indicate that $M^{\parallel}$ becomes anisotropic at very high field even in a cubic system [5], and shows an upturn above H^* when $H \| \langle 100 \rangle$. Further experimental effort is needed to examine these possibilities.

III. CONCLUSION

In summary, we have investigated the high-field phase diagram of the heavy-fermion antiferromagnet $CeIn_3$ using pulsed-field NMR up to 56 T. Within the AFM phase near $H^* = 45$ T, a field-induced anomaly has been detected in TDO measurements. The anomaly is associated with a Fermi surface reconstruction, and has been discussed as the consequence of a Lifshitz transition or a metamagnetic transition, both of which can be driven by strong magnetic field. However, we have not detected any visible change in our pulsed-field NMR spectra that could suggest a modification either in the character of the hyperfine field or in the electric field gradient at In sites. Thus, the 45 T anomaly cannot be simply ascribed to a field-induced change of magnetic structure above H^*. Our results also exclude the possibility of a substantial crystal distortion above H^*. However, since the resolution of the pulsed-field NMR spectra was not high enough, the data do not exclude a possibility of a density-wave-type [11,27] (or a nematic-type [28]) phase transition around H^*. On the other hand, our results are rather compatible with the recently proposed scenario of the field-induced level crossing around H^* [5].

We emphasize that our success in pulsed-field NMR measurements on metallic single crystals at low temperatures opens a way to investigate *microscopically* the heavy-fermion states at high magnetic fields. An interesting future direction is to examine whether similar NMR data are obtained around 45 T in $CePt_2In_7$, which exhibits a high-field phase diagram similar to $CeIn_3$, including H^*.

ACKNOWLEDGMENTS

We are grateful for stimulating discussions with R. E. Walstedt and S. Watanabe. This work was supported by JSPS KAKENHI Grants No. 26400375, No. JP15H05745, No. JP15K06884, No. JP15K21732, No. JP16H04006, No. JP15H05882, and No. JP15K05884 (J-Physics), ERC starting grant (NewHeavyFermion), ICC-IMR, the REIMEI Research Program of JAEA, and ANR-DFG grant "Fermi-NESt."

[1] N. D. Mathur, F. M. Grosche, S. R. Julian, I. R. Walker, D. M. Freye, R. K. W. Haselwimmer, and G. G. Lonzarich, Nature (London) **394**, 39 (1998).

[2] In Ref. [1] Mathur *et al.* note that the Ce ions in $CeIn_3$ are in a simple cubic array, while the In ions are located in the centers of each face of the cubic unit cell. In the AFM state the ordered Ce moments lie along the (111) axis.

[3] T. Ebihara, N. Harrison, M. Jaime, S. Uji, and J. C. Lashley, Phys. Rev. Lett. **93**, 246401 (2004).

[4] N. Harrison, S. E. Sebastian, C. H. Mielke, A. Paris, M. J. Gordon, C. A. Swenson, D. G. Rickel, M. D. Pacheco, P. F. Ruminer, J. B. Schillig, J. R. Sims, A. H. Lacerda, M.-T. Suzuki, H. Harima, and T. Ebihara, Phys. Rev. Lett. **99**, 056401 (2007).

[5] P. J. W. Moll, T. Helm, S.-S. Zhang, C. D. Batista, N. Harrison, R. D. McDonald, L. E. Winter, B. J. Ramshaw, M. K. Chan, F. F. Balakirev, B. Batlogg, E. D. Bauer, and F. Ronning, npj Quant. Mater. **2**, 46 (2017).

[6] K. M. Purcell, D. Graf, M. Kano, J. Bourg, E. C. Palm, T. Murphy, R. McDonald, C. H. Mielke, M. M. Altarawneh, C. Petrovic, R. Hu, T. Ebihara, J. Cooley, P. Schlottmann, and S. W. Tozer, Phys. Rev. B **79**, 214428 (2009).

[7] S. E. Sebastian, N. Harrison, M. M. Altarawneh, C. H. Mielke, R. Liang, D. A. Bonn, and G. G. Lonzarich, Proc. Natl. Acad. Sci. USA **106**, 7741 (2009).

[8] R. Settai, T. Kubo, T. Shiromoto, D. Honda, H. Shishido, K. Sugiyama, Y. Haga, T. D. Matsuda, K. Betsuyaku, H. Harima, T. C. Kobayashi, and Y. Ōnuki, J. Phys. Soc. Jpn. **74**, 3016 (2005).

[9] M. M. Altarawneh, N. Harrison, R. D. McDonald, F. F. Balakirev, C. H. Mielke, P. H. Tobash, J.-X. Zhu, J. D. Thompson, F. Ronning, and E. D. Bauer, Phys. Rev. B **83**, 081103(R) (2011).

[10] M. Raba *et al.* (unpublished).

[11] P. J. W. Moll, P. Kushwaha, N. Nandi, B. Schmidt, and A. P. Mackenzie, Nat. Commun. **6**, 6663 (2015).

[12] Y. Kohori, Y. Inoue, T. Kohara, G. Tomka, and P. C. Riedi, Physica B **259-261**, 103 (1999).

[13] Y. Kohori, T. Kohara, Y. Yamato, G. Tomka, and P. C. Riedi, Physica B **281-282**, 12 (2000).

[14] S. Kawasaki, T. Mito, Y. Kawasaki, G.-Q. Zheng, Y. Kitaoka, H. Shishido, S. Araki, R. Settai, and Y. Ōnuki, Phys. Rev. B **66**, 054521 (2002).

[15] S. Kawasaki, M. Yashima, Y. Kitaoka, K. Takeda, K. Shimizu, Y. Oishi, M. Takata, T. C. Kobayashi, H. Harima, S. Araki, H. Shishido, R. Settai, and Y. Ōnuki, Phys. Rev. B **77**, 064508 (2008).

[16] P. Morin, C. Vettier, J. Flouquet, M. Konczykowski, Y. Lassailly, J.-M. Mignot, and U. Welp, J. Low Temp. Phys. **70**, 377 (1988).

[17] N. J. Curro, New J. Phys. **8**, 173 (2006).

[18] J. Haase, D. Eckert, H. Siegel, H. Eschrig, K. H. Muller, and F. Steglich, Solid State Nucl. Magn. Reson. **23**, 263 (2003).

[19] G.-Q. Zheng, K. Katayama, M. Ishiyama, S. Kawasaki, N. Nishihagi, S. Kimura, M. Hagiwara, and K. Kindo, J. Phys. Soc. Jpn. **78**, 095001 (2009).

[20] E. Abou-Hamad, P. Bontemps, and G. L. J. A. Rikken, Solid State Nucl. Magn. Reson. **40**, 42 (2011).

[21] B. Meier, S. Greiser, J. Haase, T. Herrmannsdörfer, F. Wolff-Fabris, and J. Wosnitza, J. Magn. Reson. **210**, 1 (2011).

[22] H. Stork, P. Bontemps, and G. L. J. A. Rikken, J. Magn. Reson. **234**, 30 (2013).

[23] J. Kohlrautz, S. Reichardt, E. L. Green, H. Kühne, J. Wosnitza, and J. Haase, J. Magn. Reson. **263**, 1 (2016).

[24] A. Orlova, P. Frings, M. Suleiman, and G. L. J. A. Rikken, J. Magn. Reson. **268**, 82 (2016).

[25] J. Kohlrautz, J. Haase, E. L. Green, Z. T. Zhang, J. Wosnitza, T. Herrmannsdörfer, H. A. Dabkowska, B. D. Gaulin, R. Stern, and H. Kühne, J. Magn. Reson. **271**, 52 (2016).

[26] G. C. Carter, L. H. Bennett, and D. J. Kahan, *Metallic Shifts in NMR*, Progress in Materials Science (Pergamon, Oxford, 1977), Vol. 20.

[27] T. Wu, H. Mayaffre, S. Krämer, M. Horvatić, C. Berthier, W. N. Hardy, R. Liang, D. A. Bonn, and M.-H. Julien, Nature (London) **477**, 191 (2011).

[28] F. Ronning, T. Helm, K. R. Shirer, M. D. Bachmann, L. Balicas, M. K. Chan, B. J. Ramshaw, R. D. McDonald, F. F. Balakirev, M. Jaime, E. D. Bauer, and P. J. W. Mol, Nature (London) **548**, 313 (2017).